

## SOLID STATE NMR CHARACTERIZATION OF THE THERMAL TRANSFORMATION OF AN ILLITE-RICH CLAY

G. E. ROCH,<sup>1</sup> M. E. SMITH<sup>1</sup>† AND S. R. DRACHMAN<sup>2</sup>

<sup>1</sup> School of Physical Sciences, University of Kent, Canterbury, Kent, CT2 7NR, United Kingdom

<sup>2</sup> RBB Research and Development, Graylands, Langhurstwood Road, Horsham, West Sussex, RH12 4QG, United Kingdom

**Abstract**—Lode, a dioctahedral illite-rich clay from Latvia belonging to the mica group of clay minerals, undergoes thermal transformation via a series of structurally disordered intermediate phases. Despite containing high levels of paramagnetic Fe substituted into the octahedral sites, <sup>29</sup>Si and <sup>27</sup>Al magic angle spinning nuclear magnetic resonance (MAS NMR) spectra of sufficient quality are obtained to resolve different structural units, showing clearly defined structural changes which occur in the sample during calcination to 1200 °C. However, Fe plays a significant role in broadening the Al signal, with integrated peak intensities decreasing as temperature increases. Significant differences are revealed in the thermal decomposition process by NMR spectra between pyrophyllite, Ca-montmorillonite and illite clays, possibly due to the different cations present in the interlayer. It has also been shown for illite that no structural differences at the atomic level occur when the dwell time at a particular temperature is varied and no difference is observed between samples that have different thermal histories; however, a minor effect of particle size and surface area is visible in the NMR data.

**Key Words**—Illite, Iron, Paramagnetic Center, Solid-State NMR, Thermal Transformation.

### INTRODUCTION

The thermal decomposition processes occurring in clays have been studied for well over a hundred years, in order to gain an understanding of the structural changes that occur during firing and thereby help with the production of ceramic products (Grim and Bradley 1940; Earley et al. 1953; Wardle and Brindley 1972; Drits et al. 1995).

A significant proportion of the clay mineral content of Lode is illite and this is structurally related to the mica family (Worrall 1986). The term “illite” was proposed by the geologists R. E. Grim and W. F. Bradley (Grim and Bradley 1940) as a general term given to a mixture of minerals including muscovite and feldspar (Deer et al. 1992) whose physical properties resemble those of the mica family. They have no expanding lattice characteristics (Earnest 1991) and thus are low in water absorbency. It has been generally accepted that the main difference between mica and illite is that micas contain more K as interlayer cations, whereas illite contains more water and silica. The general formula for illite can be expressed as  $K_{1.5}Al_4(Si_{6.5},Al_{1.5})O_{20}(OH)_4$  (Deer et al. 1992). Illite has a 2:1 layer structure having a plane of octahedrally coordinated cations (gibbsite) sandwiched between 2 inward pointing sheets of tetrahedra (silica). Lode contains smectite interlayers (montmorillonite–beidellite) which are randomly interstratified. The basal spacing is therefore increased, and to some de-

gree shows the characteristics of a smectite such as swelling and cation exchange properties. I–S mixed layers, smectite layers interstratified among illite layers, are in fact the most abundant form of clay mineral (Worrall 1986).

When comparing data with previously published studies of NMR on the related 2:1 type clay minerals Ca-montmorillonite (Woessner 1989; Drachman et al. 1997; Sanchez-Soto and Perez-Rodriguez 1997) and pyrophyllite (Fitzgerald and Hamza 1996), several differences are seen. Previous studies of this family of clays revealed through techniques such as Mössbauer and solid-state NMR (Grim and Bradley 1940; Greene-Kelly 1955; Malathi et al. 1971; Ogloza and Malhotra 1989; Fitzgerald and Hamza 1996) that the main differences between illite and montmorillonite are the ion-exchange capacity, the position of Fe(III) or Fe(II) in the structure and the presence of different cations. It has also been reported (Grim and Bradley 1940) that illites have a low ion-exchange capacity of between 10–40 meq 100 g<sup>-1</sup> of clay, whereas montmorillonites, although structurally related to illite, have a considerable higher ion exchange capacity (80–150 meq 100 g<sup>-1</sup>).

In pyrophyllite, the layers that are formed are electrically neutral and thus the structure has no cation requirement (Deer et al. 1992). Although all of these clays are derived from the same structure belonging to the mica family, the differences in the thermal decomposition characteristics can be readily interpreted.

Earlier studies of illite-rich clays (Grim and Bradley 1940; Michael and McWhinnie 1989; Earnest 1991; Deer et al. 1992; Murad and Wagner 1996) using var-

† Present address and correspondence to: M. E. Smith, Department of Physics, University of Warwick, Coventry, CV4 7A1, United Kingdom.

Table 1. Chemical analysis of Lode.

Component	Content (wt%)
SiO <sub>2</sub>	67.9
TiO <sub>2</sub>	0.97
Al <sub>2</sub> O <sub>3</sub>	15.40
Fe <sub>2</sub> O <sub>3</sub>	6.31
CaO	0.23
MgO	1.31
K <sub>2</sub> O	4.35
Na <sub>2</sub> O	0.00
LOI	3.72
Total	100.2

Table 2. Mineralogical composition of Lode.

Whole rock	Lode (wt%)
Illite/Mica	49
Smectite	BDL†
Kaolinite	2
Quartz	43
Feldspar	2
Hematite	1
Siderite	4
Total	101

† BDL = below detection limit.

ious techniques such as electron spin resonance (ESR) and Mössbauer show there are 4 main reaction processes that occur on calcination: dehydration, dehydroxylation, structural breakdown and recrystallization. Interlayer water is driven off by 350–400 °C, followed by dehydroxylation between 450–700 °C and irreversible structural breakdown between 800–900 °C. The formation of spinel occurs at 900 °C and continues to increase in amount and particle size with increasing temperature. Hematite and corundum are produced at 1100 °C (Murad and Wagner 1996) and the latter dissolves in a silica-rich glass phase between 1250–1300 °C.

Multinuclear MAS NMR spectroscopy can provide detailed information on the structural arrangement at the atomic level due to its short-range nature. This technique uses the “chemical” shift to distinguish the local coordination number of the Al atom, for example (Engelhardt and Michel 1987), and determines the degree of connectivity of Si tetrahedra. The Q<sup>4</sup> species of SiO<sub>4</sub>-units, for example, will have 4 bridging oxygens with other tetrahedra, whereas, the Q<sup>2</sup> species will have just 2 such bridging oxygen bonds, and these units have very different <sup>29</sup>Si NMR chemical shifts (Engelhardt and Michel 1987).

Studies of muscovite using solid-state <sup>29</sup>Si and <sup>27</sup>Al NMR (Brown et al. 1987) showed that the dehydroxylate phase decomposes (1100 °C) by separation of the silica layers, which then combine with the cations (K<sup>+</sup>) forming a feldspar-like phase. The remainder of the structure forms a spinel,  $\gamma$ -Al<sub>2</sub>O<sub>3</sub>, which then transforms into aluminous mullite, and then corundum, and on further heating the mullite becomes more silica-rich by reacting with the feldspar-like phase. Recent MAS NMR studies have been undertaken on both halloysite (Smith et al. 1993) and montmorillonite (Drachman et al. 1997) and reveal that, on heating, dehydration of the interlayers has no effect on the structure of the layers themselves. On dehydroxylation, the gibbsite-like sheet structure becomes highly disordered, containing AlO<sub>4</sub>, AlO<sub>5</sub> and AlO<sub>6</sub> sites, and the silica-like sheet structure becomes more connected, transforming from Q<sup>3</sup> to Q<sup>4</sup>. However, as calcination proceeds, clear

differences can be seen in the <sup>27</sup>Al MAS NMR spectra between these clays.

The thermal decomposition of Lode results in several phases of a structurally disordered nature which cannot readily be observed with characterization techniques such as X-ray diffraction (XRD). The influence of high Fe-content on such NMR spectra is often uncertain, which can lead to difficulties in interpretation. In the work presented here a detailed solid-state MAS NMR study has been undertaken on heat-treated Lode (up to 1200 °C) and comparisons are made to Fuller's Earth, a Ca-montmorillonite (Drachman et al. 1997), thereby elucidating similarities and differences in the structural breakdown of these clay minerals. The NMR results reported here provide useful atomic scale information, enabling a better understanding of the thermal breakdown of Lode. The use of fast MAS, up to 15 kHz, results in improved quality <sup>27</sup>Al NMR spectra compared to many of the earlier studies of related clay minerals, giving more detailed information on the Al coordination. Despite the high Fe-content of this sample, up to 50% of the nuclei are detected and contribute to the signal, with sufficient spectral resolution to determine structural details.

## EXPERIMENTAL

### Samples and Heat Treatment

The raw material studied was a 77% illite-rich clay from Latvia. The chemical analysis is shown in Table 1, the mineral composition in Table 2 and the particle size distribution in Table 3. This study was carried out on the whole rock without any further treatment since

Table 3. Particle size distribution.

Particle size (μm)	Percentage (%)
>20	14
10–20	6
5–10	8
2–5	13
1–2	9
0.5–1	15
>0.5	33
Total	100

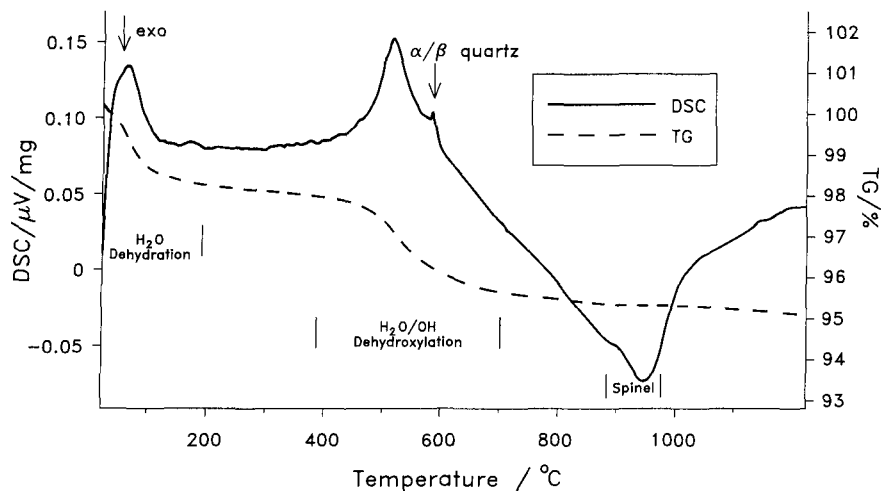


Figure 1. DTA trace from Lode heated at 20 °C/min in air.

this is the form used commercially. For a standard run, samples were ground and heated in a Carbolite STF 450 tube furnace to the indicated temperatures in a Pt crucible at a rate of 1.25 °C/min, held at temperature for 3 h and then cooled at a rate of 1.25 °C/min to room temperature (RT). Comparison was made between powdered, pressed and extruded samples to see if sample preparation had any significant influence on structural evolution with calcination. Separate samples were extruded on a Netzsch plasticimeter, and also pressed using a Norton semi-dry press. These were heated to the temperature indicated using the same parameters as the standard run. To ascertain at what time the sample reached equilibrium, samples were heated to 800 °C (this temperature was chosen since it is the onset of decomposition of the “illite” and of glass formation) at a rate of 1.25 °C/min and held there at times varying from 30 min to 48 h.

To investigate the influence of thermal history, 50 g of the sample were heated successively to the temperatures indicated in Figures 2 and 3 and cooled down, whereupon 2 g of sample were removed and analyzed (successive run). This procedure was followed to ensure that at each temperature examined the sample had undergone the same thermal history. Comparison was then made to samples taken from the standard run.

Samples were also characterized by differential thermal analysis (DTA) at a ramp rate of 20 °C/min to 1200 °C under a static air atmosphere using a Netzsch STA 409A instrument referenced to calcined kaolin. Solid-state NMR was performed on a Chemagnetics CMX 300 (7.05T) Infinity spectrometer. Performance of  $^{29}\text{Si}$  MAS NMR was accomplished using a 7.5-mm double bearing (DB) MAS NMR probe with a spinning speed of up to 5 kHz. Conditions used to collect the  $^{29}\text{Si}$  spectra were a 5- $\mu\text{s}$  ( $\sim 90^\circ$ ) pulse with a 5-s

recycle delay. The  $^{27}\text{Al}$  MAS NMR spectra were recorded using a 4-mm DB MAS probe with spinning speeds up to 15 kHz, with 1- $\mu\text{s}$  ( $\sim 15^\circ$ ) pulse and a 1-s recycle delay. These recycle delays were sufficient to ensure that the clay mineral was fully relaxed. Spectra were referenced to zeolite A at  $-89.7$  ppm for  $^{29}\text{Si}$  (Larmor frequency 59.66 MHz) and the  $\text{AlO}_6$  resonance of  $\text{Y}_3\text{Al}_5\text{O}_{12}$  at 0.7 ppm for  $^{27}\text{Al}$  (Larmor frequency 78.25 MHz). The  $^{29}\text{Si}$  spin-lattice relaxation time  $T_1$  was measured using saturation recovery. Additionally, some experiments were carried out with a pulse delay of 100 s (enough to ensure the sample had fully relaxed) to determine the effect of Fe-content on the NMR signal intensity. The integrated intensity of the Lode spectra were compared to yttrium aluminium garnet (a sample of known chemical composition having zero Fe content) for Al and pure silica for Si.

## RESULTS

Differential scanning calorimetry (DSC) results show a number of endotherms and 1 exotherm, and the thermogravimetric analysis (TG) trace shows 2 distinct weight losses (Figure 1). The total weight loss after running DSC/TG to 1200 °C was 4.9%, which is consistent with the structural water content of illite,  $\sim 5.4\%$  (Murad and Wagner 1996).

Typical  $^{29}\text{Si}$  MAS NMR spectra are shown in Figure 2 from samples heated to 400, 500, 800, 900, 1100 and 1200 °C (and 1 at RT). Below 400 °C, the spectra remain unchanged with 1 broad dominant peak at  $-92.7$  ppm (see Table 4) together with a smaller, sharper peak at  $-108.9$  ppm corresponding to quartz. MAS produces signals separated by multiples of the spinning frequency from the main resonance, termed “spinning sidebands”. In these samples, prominent spinning sidebands are observed which are a result of the paramagnetic  $\text{Fe}^{3+}$ . At RT, 2 shoulders situated off

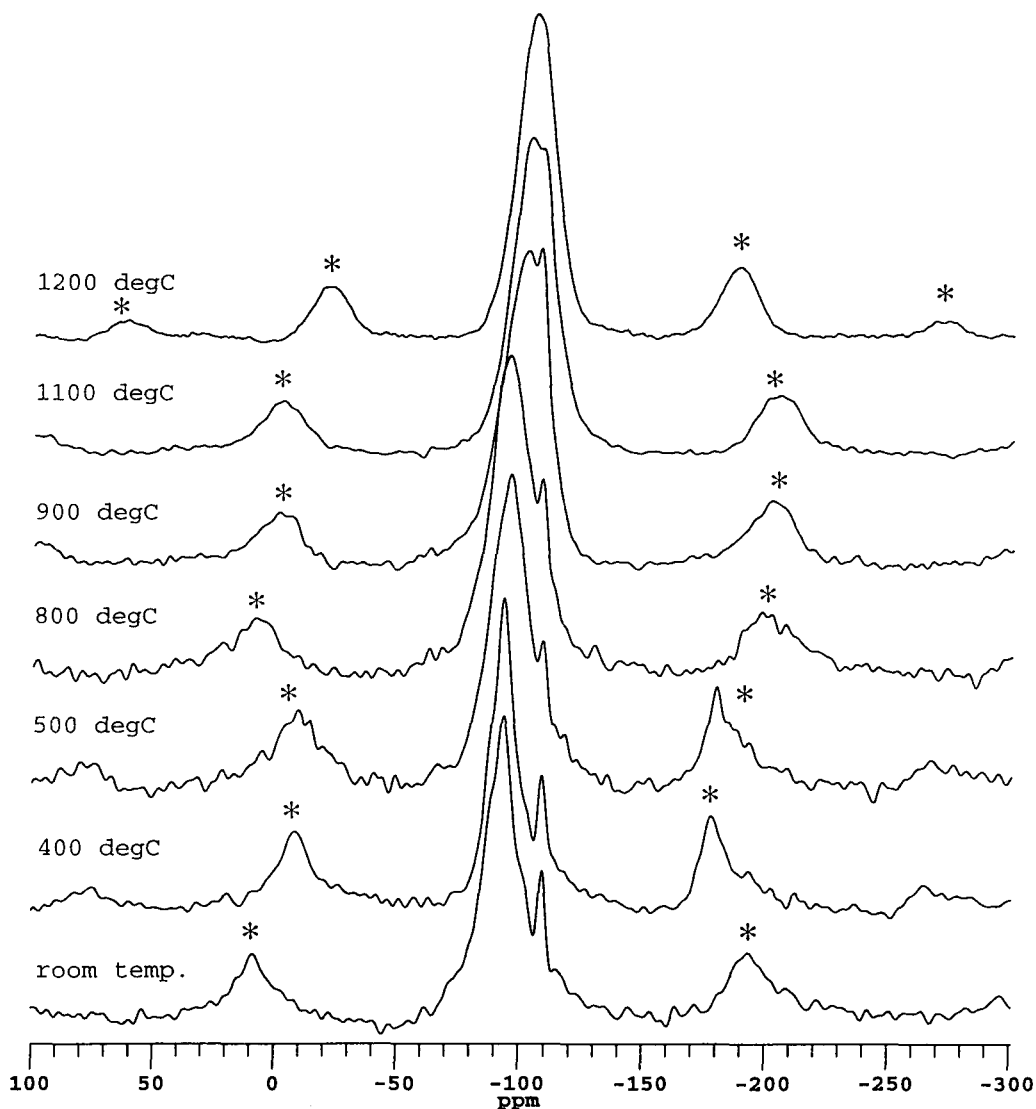


Figure 2.  $^{29}\text{Si}$  MAS NMR spectra of Lode heated at various temperatures for 3 h (\* denotes spinning sidebands).

Table 4. Summary of  $^{27}\text{Al}$  and  $^{29}\text{Si}$  MAS NMR results from the thermal decomposition of Lode.

Temperature (°C)	$^{29}\text{Si}$ peak position (ppm)	$^{27}\text{Al}$ peak position (ppm)
room	-92.9, -108.9	53.4, -1.2
100	-92.7, -108.9	51.6, -1.4
200	-92.1, -108.2	51.6, -1.4
300	-91.8, -108.1	51.8, 0.2
400	-93.2, -109.2	53.2, 1.0
500	-94.3, -108.0	51.6, 0.1
600	-95.0, -108.8	51.6, 0.1
750	-92.8, -107.9	51.8, 0.3
800	-95.6, -108.3	54.8, 0.5
850	-98.1, -107.9	52.3
900	-103.4, -108.3	50.9
950	-103.6, -108.5	47.9
1100	-102.8, -108.3	49.4
1200	-105.1	47.1

the main resonance peak can be seen which may be associated with different  $Q^3$  species, revealing the structural complexity of illite. These shoulders disappear above 400 °C. The main peak then shifts from -93.2 ppm at 400 °C to -95.6 ppm at 800 °C, to -99 ppm at 850 °C, and at 900 °C to -103.4 ppm. At 1200 °C the spectrum has changed completely, revealing only 1 broad peak at -105.1 ppm (Table 4).

Short  $T_1$ 's (<1 s) were obtained with highly non-exponential recoveries. The non-exponential recovery and fast  $^{29}\text{Si}$  relaxation, uncommon in silicates, is caused by the paramagnetic Fe(III) in the octahedral layer which is believed to be the main source of relaxation. Quantitative analysis of the effect the Fe-content has on the  $^{27}\text{Al}$  and  $^{29}\text{Si}$  signal intensity is shown in Table 5. The data reveal a decrease in signal inten-

Table 5. Effect of Fe content on  $^{27}\text{Al}$  and  $^{29}\text{Si}$  signal intensities with calcination.

Temperature (°C)	$^{27}\text{Al}$ intensity observed % ( $\pm 2\%$ )	$^{29}\text{Si}$ intensity observed % ( $\pm 2\%$ )
room	41	41
500	37	41
900	30	42
1200	22	40

sity with increasing temperature for the Al signal but no effect is observed in the Si signal. Chemical analysis revealed Lode to have 6.3 wt% of  $\text{Fe}_2\text{O}_3$ , with up to ~50% of the signal being detected. Losing 50% of the signal means that the quantitative advantage of

NMR cannot be used, so here the lineshape and shifts are used qualitatively to interpret structural changes.

The  $^{27}\text{Al}$  MAS NMR spectra are shown for samples heated to 400, 500, 700, 800, 900 and 1200 °C (and one at RT) (Figure 3). As with the  $^{29}\text{Si}$  data, no significant change in the spectra below 400 °C is observed. There is a major peak at -1.2 ppm assigned to  $\text{AlO}_6$  sites and a minor peak at 51.6 ppm assigned to  $\text{AlO}_4$  sites. There is evidence of a broader underlying resonance in the  $\text{AlO}_4$  peak which is present until 950 °C.

Changes in the spectra start to occur between 400 and 500 °C. At 500 °C, the  $\text{AlO}_4$  peak corresponding to the tetrahedral sites has increased in relative intensity. Above 600 °C, the  $\text{AlO}_6$  peak assigned to the

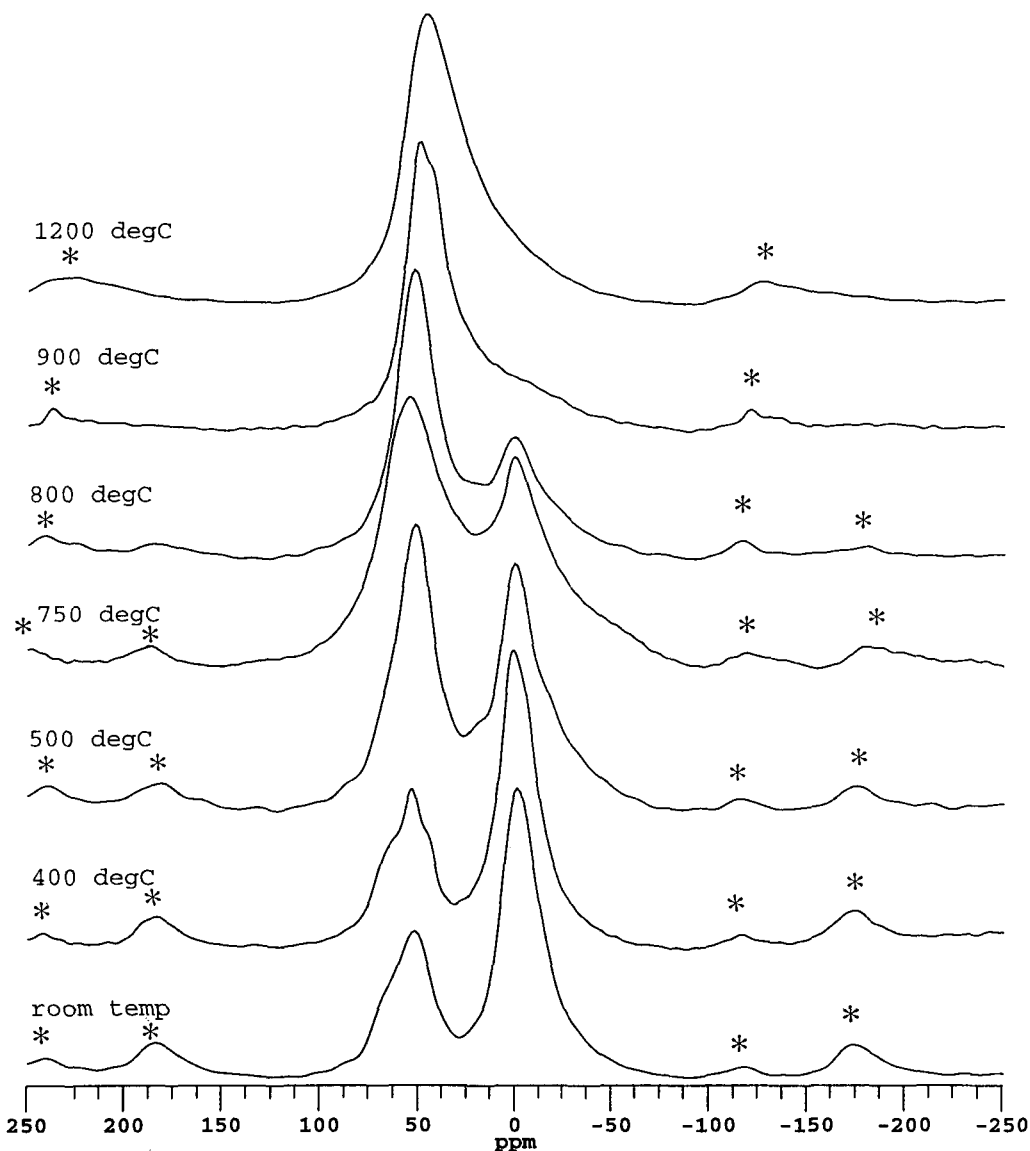


Figure 3.  $^{27}\text{Al}$  MAS NMR spectra of Lode heated at various temperatures for 3 h (\* denotes spinning sidebands).

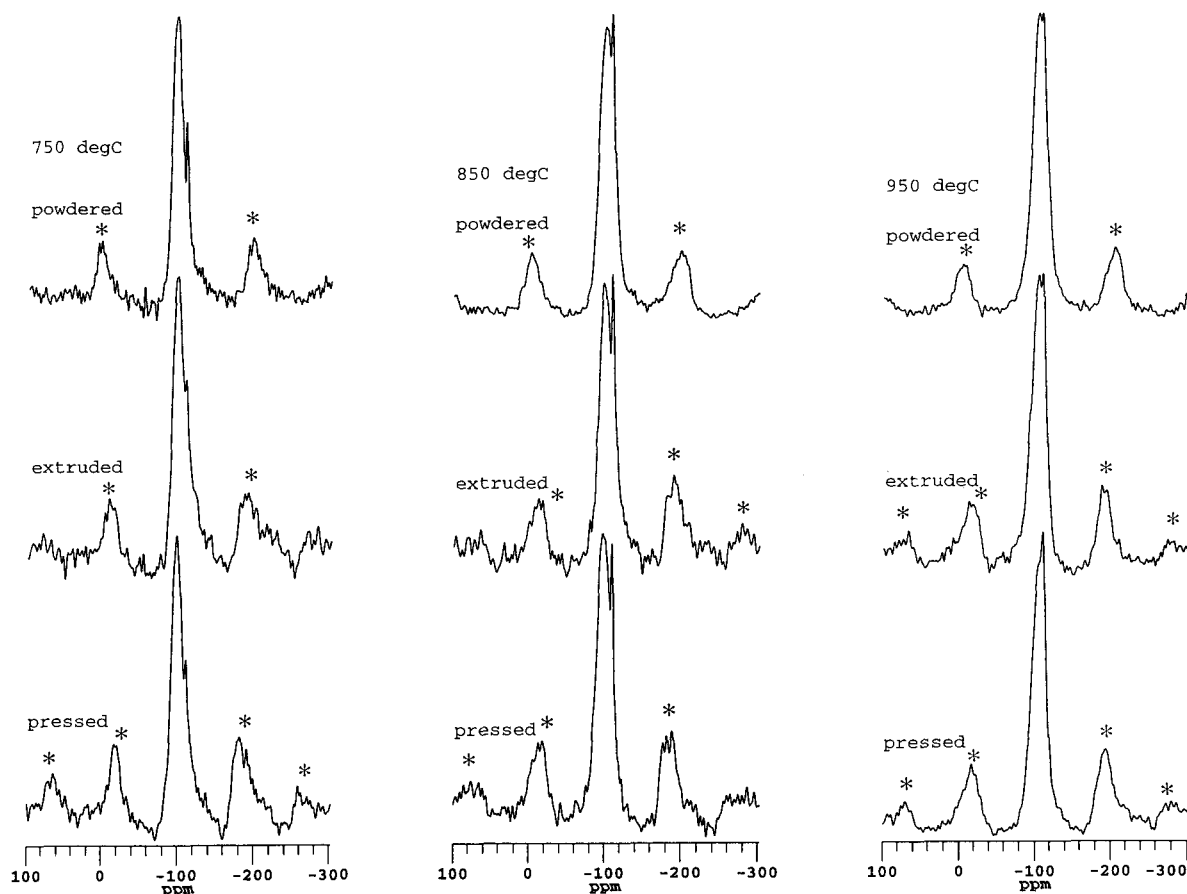


Figure 4.  $^{29}\text{Si}$  MAS NMR spectra of powdered, extruded and pressed Lode at various temperatures for 3 h (\* denotes spinning sidebands).

octahedral layers decreases in intensity until 900 °C when it has disappeared completely, leaving 1 broad peak at 50.9 ppm assigned to tetrahedrally coordinated environments. It appears that the  $\text{AlO}_4$  resonance becomes more asymmetric after 900 °C as the tail runs into the  $\text{AlO}_6$  chemical shift range. The  $^{27}\text{Al}$  NMR spectra give no evidence of  $\text{AlO}_3$  coordinations present in the intermediate phase so, although there is significant signal loss because of the presence of Fe, it is still probable that the  $\text{AlO}_3$  content of the illite dehydroxylate phase is low.

**SAMPLE PREPARATION RESULTS.** The  $^{29}\text{Si}$  and  $^{27}\text{Al}$  MAS NMR spectra are shown in Figures 4 and 5, respectively, for powdered, pressed and extruded samples at 750–950 °C, and in this temperature range no significant differences were observed between spectra from these samples. The  $^{29}\text{Si}$  MAS NMR spectra show 1 major resonance at  $\sim -94$  ppm which shifts to more negative values as the temperature increases and 1 minor resonance assigned to crystalline  $\text{SiO}_2$  at  $\sim -108$  ppm.

The  $^{27}\text{Al}$  spectra show 2 peaks, a major one at  $\sim 1$  ppm and a minor one at  $\sim 52$  ppm assigned to  $\text{AlO}_6$  and  $\text{AlO}_4$ , respectively. A difference can be seen between the pressed/extruded (no difference between this pair) and the powdered samples. At 850 °C, the pressed/extruded samples show a minor  $\text{AlO}_6$  resonance peak at  $\sim -3$  ppm; however, the powdered sample shows only 1 major peak at the same temperature,  $\sim 52$  ppm with a tail that runs into the  $\text{AlO}_6$  chemical shift range.

**SOAK TIME ANALYSIS.** From samples of Lode each heated to 800 °C for various times,  $^{27}\text{Al}$  and  $^{29}\text{Si}$  MAS NMR spectra are shown in Figure 6. No significant difference can be found between the spectra for both the  $^{27}\text{Al}$  and  $^{29}\text{Si}$  results. However, there is a subtle difference at 30 min soak time which can be seen in the  $^{27}\text{Al}$  and  $^{29}\text{Si}$  NMR spectra compared to the other soak times. The  $^{27}\text{Al}$  NMR spectra at 30 min show the minor peak at  $\sim 0$  ppm to have a higher intensity than the other soak times shown. Only a subtle difference at 30 min is seen in the  $^{29}\text{Si}$  spectra from those with

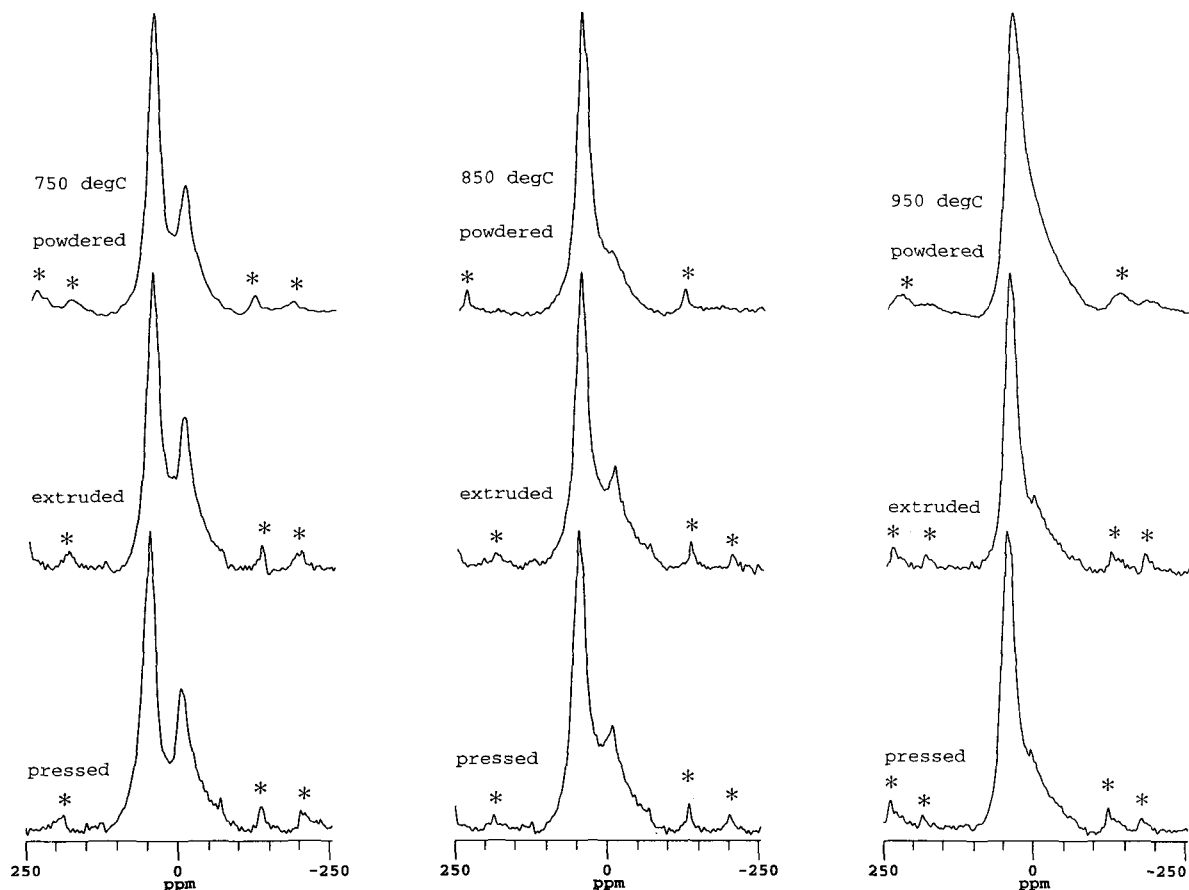


Figure 5.  $^{27}\text{Al}$  MAS NMR spectra of powdered, extruded and pressed Lode at various temperatures for 3 h (\* denotes spinning sidebands).

greater soak times. A shoulder can be seen to the left of the main resonance peak at  $\sim 95$  ppm which disappears after 30 min soak time.

**THERMAL HISTORY ANALYSIS.** The  $^{27}\text{Al}$  and  $^{29}\text{Si}$  data were collected for the temperatures indicated and  $^{29}\text{Si}$  data of samples taken from the successive runs are shown in Figure 7. Comparison of all data (that is, Figure 2 with Figure 7) reveals that there is no significant difference between samples that have seen different thermal histories and those that have experienced the same thermal history (that is, at each temperature equilibrium is achieved irrespective of the previous thermal history).

### DISCUSSION

This paper has set out to examine and understand the local structural breakdown of an illite-rich clay. However, it was initially decided to look at the effects on the NMR data of sample preparation, thermal history and soak time, to see whether they produce a difference in the structure of illite while it is being heated.

The experiments undertaken on Lode reveal that, at the atomic scale, the thermal history of the sample and the soak time after 30 min made no significant difference in the NMR signal. This ensured that heating samples for 3 h is sufficient time for equilibrium to be reached. However, having the sample pressed or extruded compared to powdered does have a very minor effect on the atomic scale structure development. Subtle differences in the  $^{27}\text{Al}$  NMR data obtained showed that pressing or extruding the samples made structural breakdown occur at a higher temperature, suggesting a greater reactivity for the more finely dispersed system. A possible explanation for this difference is in the way the water molecules that are formed can leave each powder particle on dehydroxylation. For a powdered sample, there exist many more channels for the water molecules to escape, rapidly reducing the water vapor pressure within the powder particle compared to that of pressed or extruded samples. Therefore, structural breakdown of the octahedral layer occurs more quickly in a powdered sample, with hydroxyl group loss being more rapid in comparison to pressed and

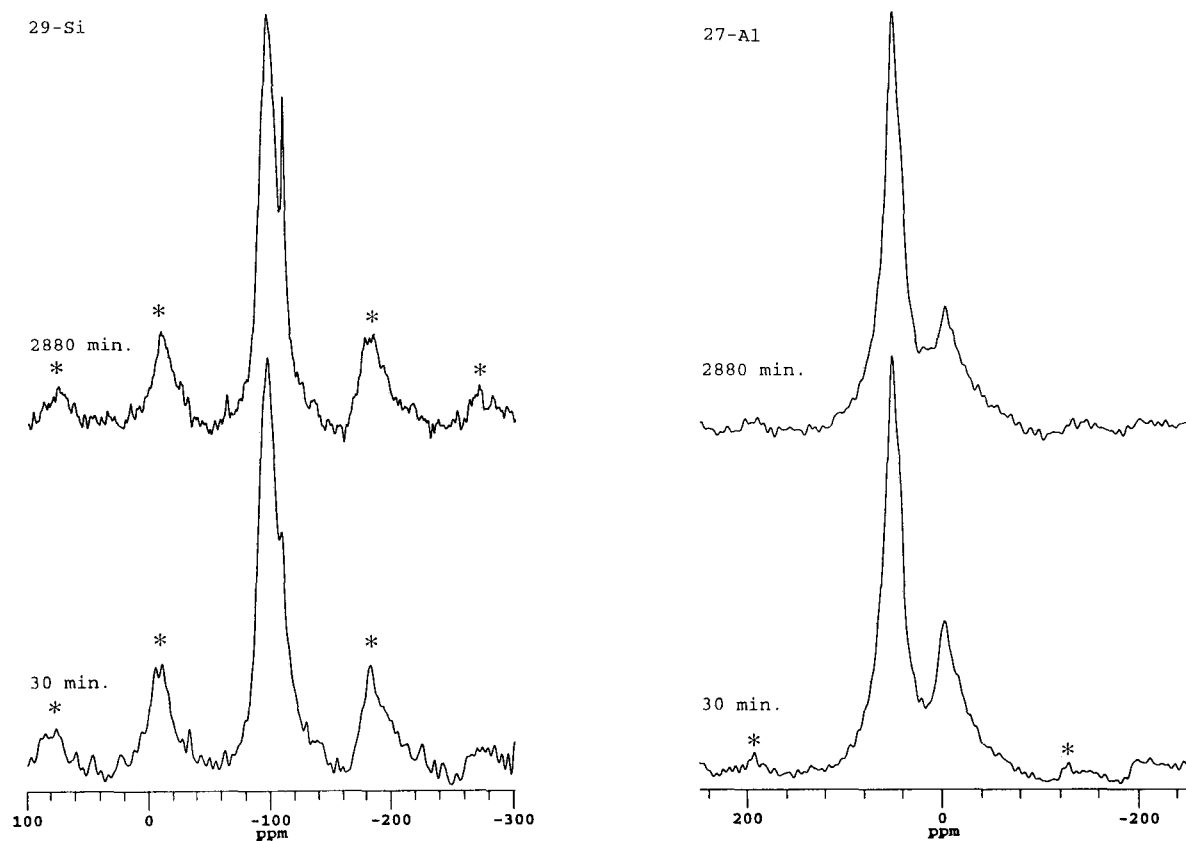


Figure 6.  $^{29}\text{Si}$  and  $^{27}\text{Al}$  MAS NMR spectra of powdered Lode heated to 800 °C for 30 and 2880 min respectively (\* denotes spinning sidebands).

extruded samples. This suggests that a higher surface area promotes a more rapid loss of water. However,  $^{29}\text{Si}$  NMR spectra for extruded, pressed and powdered samples were practically identical, which again suggests that water loss leads to the difference. This indicates that, although the rate of water loss from the octahedral layer is slightly different between these samples, the thermal breakdown of the silica layer is the same for all samples and little influenced by this water loss. This agrees with structural breakdown up to this temperature occurring mainly in the octahedral layers. Although all 3 samples undergo the same reactions, the effect of particle size and increased surface area is visible; however, illite shows little dependence on the amount of time it is being held at temperature, the thermal history it has gone through or the form in which it is heated.

The loss of  $^{27}\text{Al}$  and  $^{29}\text{Si}$  signal intensity (Table 5) shows that Fe plays a significant role in broadening some of the NMR signal. During calcination of the clay there is increasing  $^{27}\text{Al}$  signal loss, but this effect is not noticeable in the  $^{29}\text{Si}$  signal (Table 5). The presence of  $\text{Fe}^{3+}$ , because of its unpaired electron spin, will broaden the signal of nuclei close to it, such that nuclei

within 6 Å will be so broadened they cannot be observed. The possibility of the Fe being located in the tetrahedral layer is ruled out, because Si coordination sites can only accommodate ions within strict size limits (Morris et al. 1990). Therefore, although the tetrahedral layer can accommodate an  $\text{Al}^{3+}$  ion with a radius of 0.50 Å, it cannot fit an  $\text{Fe}^{3+}$  ion, which has a larger ionic radius of 0.64 Å. Thus any Fe which is absorbed in the clay structure itself will be found in the octahedral layer. If the total Fe-content present was located in the octahedral layer, *no* Al signal would be observed, since all of the Al would be within 6 Å of an  $\text{Fe}^{3+}$ . Hence, from the observed signal intensity, only about 10% of the Fe sits in the layer structure; the remainder of the Fe must be in a separate phase, such as a skin coating each particle. It should be noted that some Al atoms are substituted into the Si layer as a tetrahedrally coordinated Al peak is found at low temperatures in the  $^{27}\text{Al}$  NMR spectra shown here.

There remains the need to explain the decreasing  $^{27}\text{Al}$  signal intensity with calcination seen in Table 5. A possible solution may be that, before calcination begins, some iron is in the Fe(II) state and, as calcination proceeds, oxidation occurs to form paramagnetic



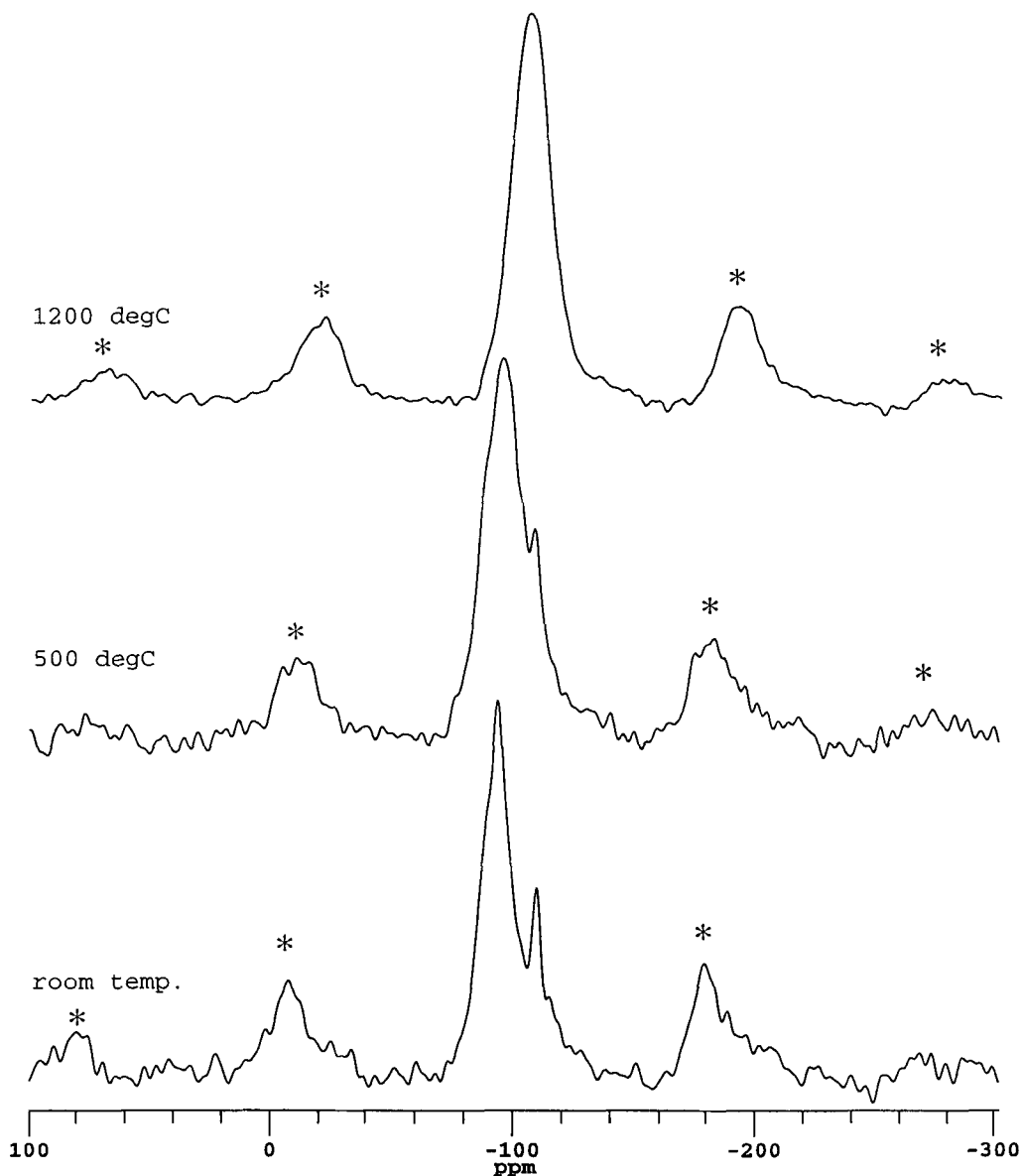


Figure 7.  $^{29}\text{Si}$  MAS NMR spectra of Lode heated to various temperatures taken from a successive run (\* denotes spinning sidebands).

Fe(III). However, Michael and McWhinnie (1989) suggested that oxidation of Fe(II) to Fe(III) is complete by 500 °C, which does not account for the continuation of decreasing signal intensity observed beyond 500 °C. Another possibility may be that the distribution of Fe(III) in the structure is also changing with temperature. The work of Schroeder and Pruett (1996) on kaolinite gave evidence that Fe exists in segregated domains in the octahedral layer. Reports that hematite is formed around 1000 °C (Michael and McWhinnie 1989; Murad and Wagner 1996) also suggests that Fe(III) is formed into clusters. However, as structural rearrangement occurs, some of the Fe(III)

could become more uniformly distributed through the aluminous phase broadening more signal from Al atoms that are now within 6 Å of an  $\text{Fe}^{3+}$  ion. It also should be noted that, given the level of Fe(III) substituted into the octahedral layer, the lack of mullite peaks is probably not due to the presence of the Fe(III) broadening all the mullite signal beyond detection.

It is clear from both the  $^{29}\text{Si}$  and  $^{27}\text{Al}$  NMR that, below 400 °C, the dehydration process that occurs in the interlayer has no effect on the NMR spectra. In the unfired clay, the spectra reveal the Si shift characteristic of  $\text{Q}^3$  sites and most of the Al is present as  $\text{AlO}_6$ . However, the  $^{27}\text{Al}$  MAS NMR spectrum indi-

ates substitution of some Al into the tetrahedral sheet, as shown by an  $\text{AlO}_4$  peak at  $\sim 53$  ppm and the  $^{29}\text{Si}$  spectra record the presence of more than one  $\text{Q}^3$  environment, revealing the complexity of the material before calcination begins. On heating, minor changes can be observed as the  $\text{Q}^3$  peak position is seen to vary between  $-92$  and  $-95$  ppm before it shifts to more negative values after heating to  $850^\circ\text{C}$ . The small shift changes before  $850^\circ\text{C}$  may be due to minor distortions in the silica layer that are associated with the dehydroxylation of gibbsite-like layers that are associated with the dehydroxylation of gibbsite-like layers that result in a change of bond angles and lengths of the silica layer. The  $\text{Q}^3$  peak splitting that was reported for the Ca-montmorillonite by Drachman et al. (1997) around  $600^\circ\text{C}$  is not evident for Lode; however, the complex nature of the structure is still evident in the spectra up until  $500^\circ\text{C}$ .

In the same temperature range,  $400$ – $500^\circ\text{C}$ , the Al spectra show a gradual decrease in intensity of the  $\text{AlO}_6$  sites, showing that the process of dehydroxylation is clearly beginning. The OH's are lost and the gibbsite-like layer is forming tetrahedral environments, evident by the increase in  $\text{AlO}_4$  intensity. There is no evidence to support the development of  $\text{AlO}_5$  as was found in the Ca-montmorillonite reported by Drachman et al. (1997), indicating the instability of the intermediate  $\text{AlO}_5$  coordination, in Lode compared to Ca-montmorillonite. There is a great variation in the stability of  $\text{AlO}_5$  in these intermediate, disordered phases with all Al becoming  $\text{AlO}_5$  in pyrophyllite, very limited formation in Ca-montmorillonite and none in Lode. The reasons for this difference may be due to the cations found in the structure, Lode's main cation being K and for fuller's earth (montmorillonite) Ca, while no cations are found in pyrophyllite. Another reason could be whether the hydroxyls in the octahedral layer are either *cis-cis* or *cis-trans* orientated, where *cis* has O-Al-OH and *trans* OH-Al-OH configurations (Brown et al. 1987).

The dehydroxylation process proceeds from  $500$ – $900^\circ\text{C}$  with some accompanying structural breakdown. At  $900^\circ\text{C}$ , the  $\text{Q}^3$  peak has shifted into the  $\text{Q}^4$  chemical shift range  $-103$  ppm, indicating that the silica layer has formed a more connected network. Also, line-broadening gives evidence that the silica layer is more structurally disordered than the initial layer. The asymmetry of the Al peak indicates disorder that results in a distribution of interactions (Smith 1993). In the  $^{27}\text{Al}$  spectra, the  $\text{AlO}_6$  peak has disappeared by  $900^\circ\text{C}$ , leaving 1 broad resonance peak at  $52.3$  ppm, indicating that all of the Al is now all tetrahedrally coordinated. At  $1200^\circ\text{C}$  there is no evidence of formation of mullite as was found with halloysite (Smith et al. 1993) and kaolinite (Sanz et al. 1988; Massiot et al. 1995; Schroeder and Pruett 1996); however,  $^{27}\text{Al}$  NMR results shown here are in

agreement with XRD studies carried out by Murad et al. Results shown here indicate that no mullite is present up to  $1200^\circ\text{C}$  and evidence suggests an aluminosilicate potassium feldspar and perhaps a separate Fe-rich spinel phase is formed (the latter would be absent from the spectrum). There is clear evidence in this report that solid-state NMR can distinguish between different clays despite the complex nature of the intermediate state, giving evidence showing differences in temperatures of the onset of dehydroxylation, structural rearrangement and breakdown into several different phases.

## CONCLUSION

Solid-state  $^{27}\text{Al}$  and  $^{29}\text{Si}$  MAS NMR together with complementary techniques such as DSC/TG and chemical analysis have shown that subtle differences can be picked up between very similar 2:1 clay minerals containing a significant amount of Fe. The  $^{27}\text{Al}$  MAS NMR spectra in particular show the gross differences between the illite-rich clay studied here and 2 others, montmorillonite (Drachman et al. 1997) and pyrophyllite (Fitzgerald and Hamza 1996), namely with respect to the amount of 5-coordinated Al in the dehydroxylate state and the absence of any mullite at high temperatures. What is believed to form from an illite-rich clay is an aluminosilicate potassium feldspar.

Quantitative analysis of the effect of Fe content reveals that the Fe found in the structure affects the Al layer more as temperature increases with the Si signal remaining largely unchanged, confirming that the Fe is indeed found in the octahedral layer. However, the presence of any Al signal indicates that the Fe is not uniformly distributed throughout the octahedral layer and is largely present as a separate phase.

Further investigations on Lode reveal that there is no significant difference in the NMR spectra between the different sample preparations discussed in this report, indicating that running experiments on powdered samples can be of direct relevance to industry.

## ACKNOWLEDGMENTS

G. Roch would like to thank EPSRC and RBB Research and Development Ltd. for the provision of a CASE studentship and MES would also like to thank NERC for partial support.

## REFERENCES

- Brown IWM, MacKenzie KJD, Meinhold RH. 1987. The thermal reactions of montmorillonite studied by high resolution solid state Si-29 and Al-27 NMR. *J Mater Sci* 22: 3265–3275.
- Deer WA, Howie RA, Zussman J. 1992. An introduction to the rock-forming minerals. Hong Kong: Longman. 720 p.
- Drachman SR, Roch GE, Smith ME. 1997. Solid state NMR characterisation of the thermal transformation of fuller's earth. *Solid State NMR* 9:257–267.
- Dritis VA, Besson G, Muller F. 1995. An improved model for structural transformations of heat-treated aluminous dioctahedral 2:1 layer silicates. *Clays Clay Miner* 43:718–731.

- Earley JW, Milne IH, McVeagh WJ. 1953. Thermal dehydration and X-ray studies on montmorillonite. *Am Mineral* 38: 770–783.
- Earnest CM. 1991. Thermal analysis of selected illite and smectite clay minerals part I: Illite clay specimens. In: *Lecture notes in earth sciences*. Berlin: Springer-Verlag. p 270–286.
- Engelhardt G, Michel D. 1987. General aspects of Si-29 and Al-27 NMR of the silicate and aluminosilicate framework. In: *High resolution solid-state NMR of silicates and zeolites*. New York: J. Wiley. p 106–155.
- Fitzgerald JJ, Hamza AI. 1996. Solid-state 27-Al and 29-Si NMR and 1-H CRAMPS studies of the thermal transformation of the 2:1 phyllosilicate pyrophyllite. *J Phys Chem* 100:17351–17360.
- Greene-Kelly R. 1955. Dehydration of the montmorillonite minerals. *Mineral Mag* 30:604–615.
- Grim RE, Bradley WF. 1940. Investigation of the effect of heat on the clay minerals illite and montmorillonite. *J Am Ceram Soc* 22:242–248.
- Malathi N, Puri SP, Saraswat IP. 1971. Mossbauer studies of iron in illite and montmorillonite. II. Thermal treatment. *J Phys Soc Jpn* 31:117–122.
- Massiot D, Dion P, Alcover J, Bergaya F. 1995. Al-27 and Si-29 MAS NMR study of kaolinite thermal decomposition by controlled rate thermal analysis. *J Am Ceram Soc* 78: 2940–2944.
- Michael PJ, McWhinnie WR. 1989. Mössbauer and ESR studies of the thermochemistry of illite and montmorillonite. *Polyhedron* 8:2709–2718.
- Morris HD, Bank S, Ellis PD. 1990. Al-27 spectroscopy of iron-bearing montmorillonite clays. *J Phys Chem* 94:3121–3129.
- Murad E, Wagner U. 1996. The thermal behaviour of an Fe-rich illite. *Clay Miner* 31:45–52.
- Ogloza AA, Malhotra VM. 1989. Dehydroxylation induced structural transformations in montmorillonite: An isothermal FTIR study. *Phys Chem Miner* 378–385.
- Sanchez-Soto PJ, Perez-Rodriguez JL. 1997. Influence of grinding in pyrophyllite-mullite thermal transformation assessed by 29-Si and 27-Al MAS NMR spectroscopies. *Chem Mater* 9:677–684.
- Sanz J, Madani A, Serratos JM. 1988. Al-27 and Si-29 MAS NMR study of the kaolinite-mullite transformation. *J Am Ceram Soc* 71:C-418–C-421.
- Schroeder PA, Pruett RJ. 1996. Fe ordering in kaolinite: Insights from Si-29 and Al-27 MAS NMR spectroscopy. *Am Mineral* 81:26–38.
- Smith ME. 1993. Application of Al-27 NMR techniques to structure determination in solids. *Appl Magn Res* 4:1–64.
- Smith ME, Neal G, Trigg MB, Drennan J. 1993. Structural characterization of the thermal transformation of halloysite by solid state NMR. *Appl Magn Res* 4:157–170.
- Wardle R, Brindley GW. 1972. The crystal structures of pyrophyllite, 1Tc and of its dehydroxylate. *Am Mineral* 57: 732–750.
- Woessner DE. 1989. Characterization of clay minerals by Al-27 NMR spectroscopy. *Am Mineral* 74:203–215.
- Worrall WE. 1986. *Clays and ceramic raw materials*. London: Elsevier.

(Received 5 January 1998; accepted 20 April 1998; Ms. 98-001)